Carbohydrate Polymers 92 (2013) 1026–1032

Contents lists available at SciVerse ScienceDirect

Carbohydrate Polymers

journal homepage: www.elsevier.com/locate/carbpol

Higher order structures of a bioactive, water-soluble (1→3)-β-D-glucan derived from *Saccharomyces cerevisiae*

Fen Qin [a], Marit Sletmoen [b], Bjørn Torger Stokke [b], Bjørn E. Christensen [a,*]

[a] NOBIPOL, Dept. of Biotechnology, The Norwegian University of Science and Technology, NTNU, NO-7491 Trondheim, Norway
[b] Biophysics and Medical Technology, Dept. of Physics, The Norwegian University of Science and Technology, NTNU, NO-7491 Trondheim, Norway

ARTICLE INFO

Article history:
Received 29 August 2012
Received in revised form 2 October 2012
Accepted 3 October 2012
Available online xxx

Keywords:
β-1,3 Glucan
Saccharomyces cerevisiae
SEC-MALLS
AFM
CM-curdlan
DLS

ABSTRACT

Water-soluble (1→3)-β-D-glucans with 1,6-linked branches (SBG), originally isolated from the cell walls of *Saccharomyces cerevisiae* and partially depolymerised to a weight average degree of polymerisation (DP_w) in the range 120–160 for optimal performance in wound healing applications, were studied by dynamic light scattering (DLS), SEC MALLS and AFM. Results indicate that dilute aqueous SBG solutions (1 μg/ml to 3 mg/ml) contain higher order structures with a very wide size distribution in water (10–500 nm), corresponding to a mixture of single chains, multi-chain aggregates including triple-stranded motifs, and particulate materials. The latter were enriched in longer chains compared to non-particulate fractions. The size distribution of SBG aggregates shifted to slightly lower values upon heating, but showed hysteresis upon cooling. AFM images prepared from very dilute aqueous solution (1–5 μg/ml) analysis showed by comparison to other (1→3)-β-D-glucans that some of the structures were the triple helical species coexisting with larger aggregates and single chains, in contrast to carboxymethylated SBG, which contained predominantly single chains. The ability to control the aggregation behaviour of SBG enables tailoring of the physical, and possibly bioactive, properties of SBG preparations.

1. Introduction

The water-soluble, branched (1→3)-β-D-glucans (SBG) that can be extracted from the cell wall of Bakers yeast (*Saccharomyces cerevisiae*) have been extensively studied (Bohn & BeMiller, 1995; Huang et al., 2012; Laugier, Spasić, Mandić, Jakovljević, & Vrvić, 2012) because of their ability to stimulate the immune system (Vetvicka, Vashishta, Saraswat-Ohri, & Vetvickova, 2008). Recently, industrial SBG based products, for example a biogel for wound treatment, have been developed. The basis for such products is SBG with intermediate chain lengths (DP_w = 120–160), intermediate polydispersity (DP_w/DP_n = 1.5–1.6) and on average 5 branches per 100 units (Qin, Aachmann, & Christensen, 2012).

SBG is structurally related to – but at the same time different from – several other plant or fungal branched (1→3)-β-D-glucans. Examples include laminarin (Read, Currie, & Bacic, 1996), schizophyllan (Yanaki et al., 1983), lentinan (Bluhm & Sarko, 1977), scleroglucan (Bluhm, Deslandes, Marchessault, Pérez, & Rinaudo, 1982), and many others (Carbonero et al., 2001; McIntosh, Stone, & Stanisich, 2005; Zhang & Yang, 1995). Despite differences in branching content or patterns, or chain length distributions, chain association in aqueous solutions is a recurrent theme. The mode of association varies, from the well defined, soluble triple helices observed in schizophyllan (Yanaki et al., 1983) and scleroglucan (Yanaki & Norisuye, 1983), the large soluble aggregates observed for SBG, to water-insoluble materials often found in many cases. Many (1→3)-β-D-glucans dissolve as single, un-associated chains at sufficiently high temperatures (McIntire & Brant, 1998), in dilute alkali (Gawronski, Park, Magee, & Conrad, 1999; Zhang, Ding, Zhang, Zhu, & Zhou, 1997), in organic solvents such as DMSO (Yanaki & Norisuye, 1983) or DMAc/LiCl (Striegel & Timpa, 1995), or in aqueous solution following carboxymethylation (Qin et al., 2012) or phosphorylation (Williams et al., 1991).

The aggregated nature of aqueous SBG preparations (typically 2% aqueous solutions) manifests itself by the presence of insoluble material, solution turbidity, high solution viscosities, distinct melting/setting behaviour upon heating/cooling as well as characteristically high molar masses, but low intrinsic viscosities and r.m.s. radii (Qin et al., 2012). Otherwise, little is known about the nature of the SBG aggregates found in preparations optimised for biological activity, although it seems generally accepted (Palma et al., 2006) that some degree of chain association is indeed needed to activate glucan receptors, and therefore a preferred property.

Here we present novel data for dilute SBG solutions based on dynamic light scattering (DLS) and tapping mode atomic force microscopy (AFM) measurements demonstrating that solutions contain a mixture of single chains, triple-stranded species, as well as larger structures and particulate components.

* Corresponding author. Tel.: +47 73593327; fax: +47 73591283.
E-mail address: bjorn.christensen@biotech.ntnu.no (B.E. Christensen).

0144-8617/$ – see front matter © 2012 Elsevier Ltd. All rights reserved.
http://dx.doi.org/10.1016/j.carbpol.2012.10.013

Table 1
Weight (DP_w) and number (DP_n) average degrees of polymerisation of SBG batches used in the present work. Values were obtained by aqueous SEC-MALLS of the carboxymethylated derivatives (DS = 0.23–0.91).

Sample	DP_w	DP_n	DP_w/DP_n
221-7	143	92	1.55
321-5 HMW	212	158	1.34
131-9	144	93	1.55

DLS provides the hydrodynamic radius distribution and can for example monitor changes of the macromolecular or aggregate size in the process of warming and cooling. This line of ensemble average information is complemented by ultramicroscopic investigation using tapping mode atomic force microscopy (AFM) (Falch & Stokke, 2001). All samples were prepared for AFM observations using drying procedures previously reported to preserve relevant information on chain stiffness (Stokke & Brant, 1990).

We further demonstrate by means of SEC-MALLS that particulate materials present in SBG solutions are enriched in high molecular weight chains compared to soluble species.

As a basis of comparison we include measurements of triple-stranded scleroglucan, carboxymethylated SBG (CM-SBG) and carboxymethyl curdlan (CM-curdlan).

2. Materials and methods

2.1. Samples

SBG batches 221-7 (freeze-dried), 321-5 HMW and 131-9 (both 20 mg/ml aqueous solutions) were obtained from Biotec Pharmacon ASA, Tromsø, Norway. Their chain lengths based on aqueous SEC-MALLS for carboxymethylated derivatives (Qin et al., 2012) are given in Table 1.

CM-SBG with degree of substitution (DS) of 0.91 was derived from SBG 221-7 as described previously (Qin et al., 2012). CM-curdlan (DS = 0.4) was obtained from Megazyme International, Ireland. Scleroglucan (Actigum CS11) was a laboratory sample originally obtained from Sanofi, France.

Sclerox-60 (partially carboxylated scleroglucan) was a laboratory sample. Its preparation and properties have been described previously (Guo, Elgsaeter, Christensen, & Stokke, 1998).

All samples were dried in vacuo over P_2O_5 before use.

2.2. Sample preparation

SBG solutions were prepared for DLS as described earlier (Qin et al., 2012). In brief, solutions (20 mg/ml in pure water) were first heated to 50 °C and diluted with water to 0.4 mg/ml or 0.8 mg/ml. They were further kept at 50 °C for 40 min prior to centrifugation using a Beckman Coulter Avanti® J-30I High-performance centrifuge at 27,216 × *g* at 40 °C for up to 270 min. The supernatants were kept at 50 °C prior to analysis.

Alternatively, SBG solutions were prepared for DLS measurements by using the procedure developed for SEC-MALLS analyses (Qin et al., 2012). In brief, SBG was dissolved in 0.05 M Na_2SO_4/0.01 M EDTA (pH 6) (1–3 mg/ml), and heated at 100 °C for 15 min. The solutions were cooled to room temperature, filtered (0.45 μm) and analysed by DLS (ALV instrument) at 20 °C.

2.3. Dynamic light scattering (DLS)

The size of SBG in aqueous solution was determined by dynamic light scattering using a Zetasizer nano ZS (Malvern Instruments, UK) with a detection angle of 173°. SBG aqueous solution (0.1 mg/ml) were prepared and kept at different temperatures (RT and 50 °C). The solutions filtered (0.22 μm) before the measurements at 25 °C and 50 °C, respectively. At least 5 separate measurements were performed on each the sample to ensure stable results. The size distribution of SBG is expressed as the intensity and volume distribution obtained from analysis of the correlation function. Dispersion Technology Software (DTS) (V6.20) was used for data collection and analysis.

Alternatively, DLS measurements were carried out on an ALV5000 digital correlator and ALV 5022F goniometer (ALV, Germany), and a 22 mW HeNe laser operated at a wavelength of 632.8 nm and a scattering angle of 90°. Samples were subjected to a heating and cooling cycle in the temperature range 20–55 °C with 5 °C intervals and a 5 min equilibration time at each temperature. The duration of each measurement was typically 60 s and results were averaged over a minimum number of two runs.

2.4. AFM

Tapping mode atomic force microscopy was carried out using a Digitial Instruments Multimod2e IIIa AFM (Santa Barbara, CA, USA) equipped with an E-scanner under ambient conditions. Tapping mode silicone nitride cantilevers PPP-NCH (Nanosensors, Neuchatel, Switzerland) with nominal resonance frequencies of 204–497 N/m were employed. Overlapping of trace and retrace signals were used as a prerequisite for adequate image acquisition. The topographs were obtained at scan sizes in the range from 1 μm × 1 μm to 5 μm × 5 μm (2048 × 2048 pixels) and flattened line by line.

The procedure for samples preparation for AFM has been reported (Stokke, Falch, & Dentini, 2001). Briefly, 60% glycerol solution mixed with aliquots of the well dissolved polymer solution (1 mg/ml) to a final concentration of 1–5 μg/ml. 50–100 μl of these solutions was sprayed by Nitrogen on freshly cleaved mica discs and vacuum dried at 10^{-6} Torr for at least 4 h.

The topographs from AFM were analysed by employing a user-interactive software developed in the IDL language (Research System, Inc., Boulder, CO, USA) similar to what has been described by others (Fang et al., 1998).

2.5. SEC-MALLS

The chain length distribution of fully dissociated (unaggregated) SBG was determined by SEC-MALLS with 0.5% LiCl in dimethyl acetamide (DMAc) as eluent, based on a method originally developed for cellulose (Striegel & Timpa, 1996). The separation was performed on three serially connected Mixed-A columns (particle diameter 20 μm) (Polymer Laboratories) with a guard column (Polymer Laboratories) at 1 ml/min flow rate. The detection system consisted of a DAWN DSP multi-angle laser light scattering (MALLS) detector at 633 nm (Wyatt Technology, USA), and an Optilab DSP (Wyatt Technology, USA) or Shodex RI SE-61 (Japan) differential refractometers. The MALLS instrument was normalised with 30 kDa polystyrene (Polymer Laboratories) and data acquisition was carried out with ASTRA software version 4.70 or 5.3.14 (Wyatt Technology, USA). A refractive index increment (dn/dc) of 0.12 ml/g was used on the basis of a separate experiment (unpublished data).

3. Results

3.1. Temperature dependence on the hydrodynamic radius distribution of SBG studied by dynamic light scattering

SBG was diluted to 1 mg/ml and analysed by DLS across a heating–cooling cycle (20 °C–55 °C–20 °C). Applying a deconvolution analysis of the autocorrelation function (CONTIN) resulted in

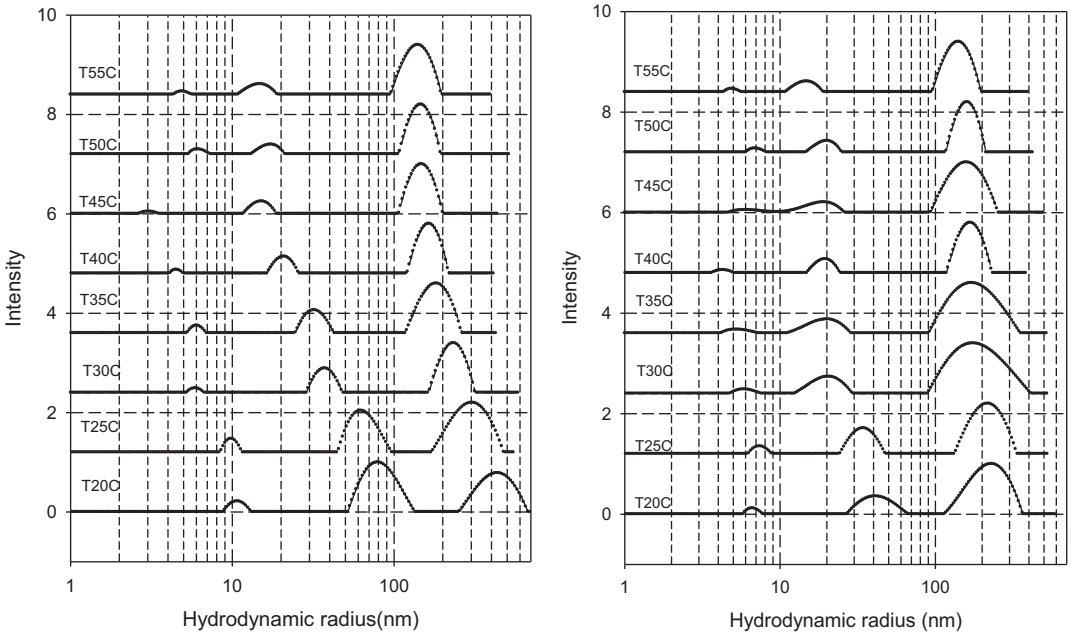

Fig. 1. Intensity distribution of the hydrodynamic radius obtained from CONTIN analyses of the dynamic light scattering data for SBG 221-7 solution (1 mg/ml) determined at a scattering angle 90° for increasing (A) and decreasing (B), respectively, temperatures in the range of 20–55 °C. Intensity on the left axis refers to the relative percentage of particles in each class based on the intensity of light scattered at the scattering angle 90°.

spectra of time constants. These were further converted to the corresponding hydrodynamic radius distribution. Results are shown in Fig. 1. The main observation is that the size distribution shifts to smaller hydrodynamic radius upon heating and apparently levels off at about 130 nm (main peak) when the temperature approaches 50 °C. However, the hydrodynamic radii distributions of the SBG sample shows hysteresis as evident from lack of return to the initial state just after being cooled to 20 °C. The results suggest that the largest aggregates dissociate irreversibly upon heating. These findings are in excellent agreement with previous observations of the melting/gelation behaviour of 2% SBG solutions observed by rheological measurements (Qin et al., 2012).

Although the CONTIN method tends to provide 'artificial' multimodal distributions, the data suggest that small particles with hydrodynamic radii (R_h) in the range 10–20 nm co-exist with the larger particles. This is at variance with a more continuous distribution as expected from the SEC-MALLS data. On the other hand the 10–20 nm size range is in qualitatively good agreement with previous SEC-MALLS analysis of unheated (but strongly diluted) SBG, which show a low molecular weight tail (M_w < 100 kDa) where the r.m.s. radius (R_G) is below 20 nm. Normally, R_G/R_h is less than 2 except for rigid rods (Burchard, 1991) and the qualitative comparison therefore holds. This fraction is enriched when the analysis is carried out at high temperature (Qin et al., 2012). However, the size of the larger components indicates a large portion of the sample is still aggregated at high temperature (55 °C), again in excellent agreement with SEC-MALLS data.

3.2. Influence of centrifugation on the hydrodynamic radius distribution of SBG

Previous results had shown that up to 5–15% of the SBG could be removed by dilution to 0.4 mg/ml followed by centrifugation at 27,216 × *g* at 40 °C for 270 min (Qin et al., 2012). The solid-free supernatant was therefore analysed by DLS at 25 °C and 50 °C, respectively. Typically, the samples were observed to possess bimodal distributions of apparent hydrodynamic radii as shown in Fig. 2.

There is a clear dependence on the temperature since most, but not all, of the larger aggregates seem to have dissociated at 50 °C.

Compared to the results in Fig. 1 the removal of larger particles clearly shifted the distribution towards smaller radii, with the

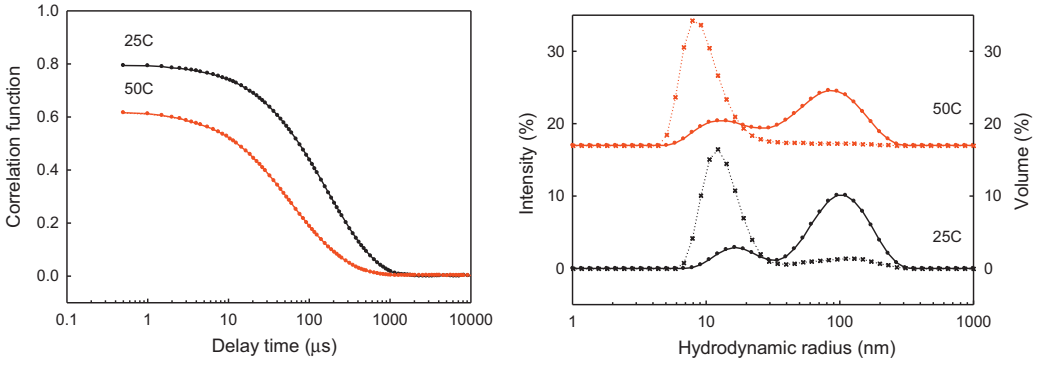

Fig. 2. DLS results obtained for heat-treated (40 °C) and centrifuged SBG (diluted to 0.1 mg/ml). (A) Correlation function and (B) CONTIN analysis of DLS spectra. Curves with line and dots (–•–) refer to the relative percentage of particles in each class based on the intensity of light scattered (left axis), whereas the curves with dotted line and cross (···×···) refer to the relative percentage of particles in each class based on the volume occupied (right axis).

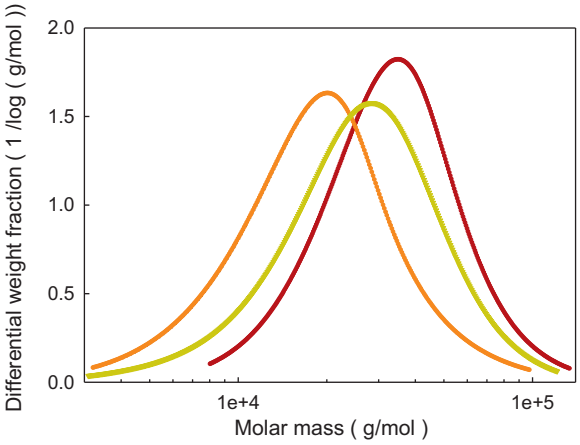

Fig. 3. Molar mass distributions (obtained by SEC-MALLS in DMAc/LiCl) of uncentrifuged SBG (green) and the precipitate (brown) and the supernatant (orange) following centrifugation of dilute SBG at 40 °C. (For interpretation of the references to colour in this figure legend, the reader is referred to the web version of the article.)

major peak in the range 100 nm. Yet, such sizes must correspond to aggregated chains considering the chain length distribution of the individual chains in SBG (see below).

3.3. Chain length distributions of the soluble and the particulate fractions following centrifugation

The recent development of SEC-MALLS analysis of SBG using DMAc/LiCl as solvent allows analysis of the chain length distribution of individual SBG chains irrespective of their physical state, i.e. whether they are single chains or multi-stranded, or particulate structures, without carboxymethylation. A full account of the method will be published in a forthcoming article. Fig. 3 shows results obtained for SBG before and after centrifugation at 40 °C.

It is clearly observed that the precipitate is enriched in chains of higher molar masses, whereas the supernatant is enriched in shorter chains. Hence, the tendency for aggregation and precipitation depends as expected on the chain length, although it remains currently unclear whether the fractionation also reflects differences in branching patterns as observed, for instance, in laminarins with different solubilities (Read et al., 1996).

3.4. AFM measurements

Tapping mode AFM images of SBG and relevant reference substances prepared in aqueous solution are shown in Fig. 4. Representative cross-sectional profiles (heights above the surfaces) are given in Fig. 5.

SBG reveals primarily rod-like structures with uniform heights along the contour and lengths in the range 20–100 nm (Fig. 4a). A tendency to form slightly curved species observed in larger abundance for the longer chains are considered to be in qualitative agreement with a wormlike polymer model. In addition, there are examples of apparently branched species. These were associated with increasing heights at the branch points (data not shown), suggesting they are mainly overlapping chains. The cross-sections (Fig. 5a) show that most of the rod-like species have heights above mica surface in the range 0.5 nm, although values up to 1.0 nm are seen occasionally. In contrast, data obtained for carboxymethylated SBG (CM-SBG, DS of 0.91) (Figs. 4b and 5b) reveal only isolated dots with lateral dimension significantly smaller than the range observed for the unmodified SBG. This modified SBG has previously been reported to behave as unaggregated random coils in solution (Qin et al., 2012), which can explain the appearance determined by AFM.

These results for SBG are quite similar to those obtained for sclerox-60 (Figs. 4c and 5c), which is also triple-stranded (Stokke et al., 2001). Further, the data are similar to those previously for triple-stranded scleroglucan (Stokke et al., 2001).

We included AFM imaging of CM-curdlan (DS = 0.4, Figs. 4d, e and 5d, e) as an additional basis of comparison. Characterisation of the CM-curdlan and CM-SBG by SEC-MALLS is reported to yield similar behaviour, i.e. single-stranded random coils (Qin et al., 2012). CM-curdlan in water (Fig. 4d) appears in AFM as flexible chains, which lengths up to 500 nm. The AFM topographs of the CM-curdlan indicate thin strands interconnecting more condensed domains, that to some extent resemble a polyelectrolyte in a poor solvent with partial collapsed domains (Kiriy et al., 2002).

4. Discussion

4.1. Association modes of SBG

Several (1→3)-β-D-glucans have the ability to form ordered structures based on a triple-stranded motif. It is generally assumed the motif corresponds to the triple-helix originally described for curdlan in the solid (crystalline) state (Deslandes, Marchessault, & Sarko, 1980). The triple-helix is characterised by having side-chains oriented towards the exterior (Bluhm et al., 1982), which requires a regular distribution of side-chains as found, for example, in schizophyllan and scleroglucan. The precise distribution pattern of side chains in SBG is unknown, but the low content of side chains (typically 5%) necessarily allows for long unsubstituted regions, which in principle could form triple helices. If the side-chains additionally are positioned so that they point outwards the triple helices may not necessarily be destabilised by branching. The ability to form triple helices has also been shown to depend on the chain length of the individual chains. In the schizophyllan case triple helices dominated when M_w was larger than approximately 9×10^4 Da, and that triple helices and single chains co-existed, with a monotonously decreasing proportion of the former, when M_w decreased towards 5×10^3 Da, below which all chains were single-stranded (Yanaki & Norisuye, 1983). The chain length distribution of SBG (Fig. 3) lies almost entirely within the molecular weight interval where single-stranded and triple-stranded structures are reported to co-exist in solution in the case of regularly comb-like branched β-D-glucans.

The temperature-dependence of the particle size distribution and the hysteresis observed for SBG solutions using DLS (Figs. 1 and 2) further suggests that triple helices co-exist with disordered chains (Sletmoen & Stokke, 2008). The presence of particulate material revealed by centrifugation further suggests that SBG also contains larger structures most likely formed by chain association.

The presence of triple-stranded species in SBG is further be supported by the AFM micrographs (Figs. 4a and 5a). First, rod-like structures in AFM images similar to those of scleroglucan and sclerox-60 are observed (McIntire & Brant, 1998; Sletmoen, Christensen, & Stokke, 2005; Stokke et al., 2001), which certainly contrast the coil-like species observed for single-stranded CM-SBG. Secondly, the height profiles across the rods are further in good agreement with triple strands (McIntire & Brant, 1998; Stokke et al., 2001). Our absolute values for heights are slightly less than those previously reported for sclerox-60 and scleroglucan, possibly arising from exerting different forces on the samples in the two cases.

A system closely related SBG is PGG-glucan, which on the basis of small angle X-ray scattering (SAXS) measurements and SEC-MALLS (including post-column denaturation in alkali) has been described

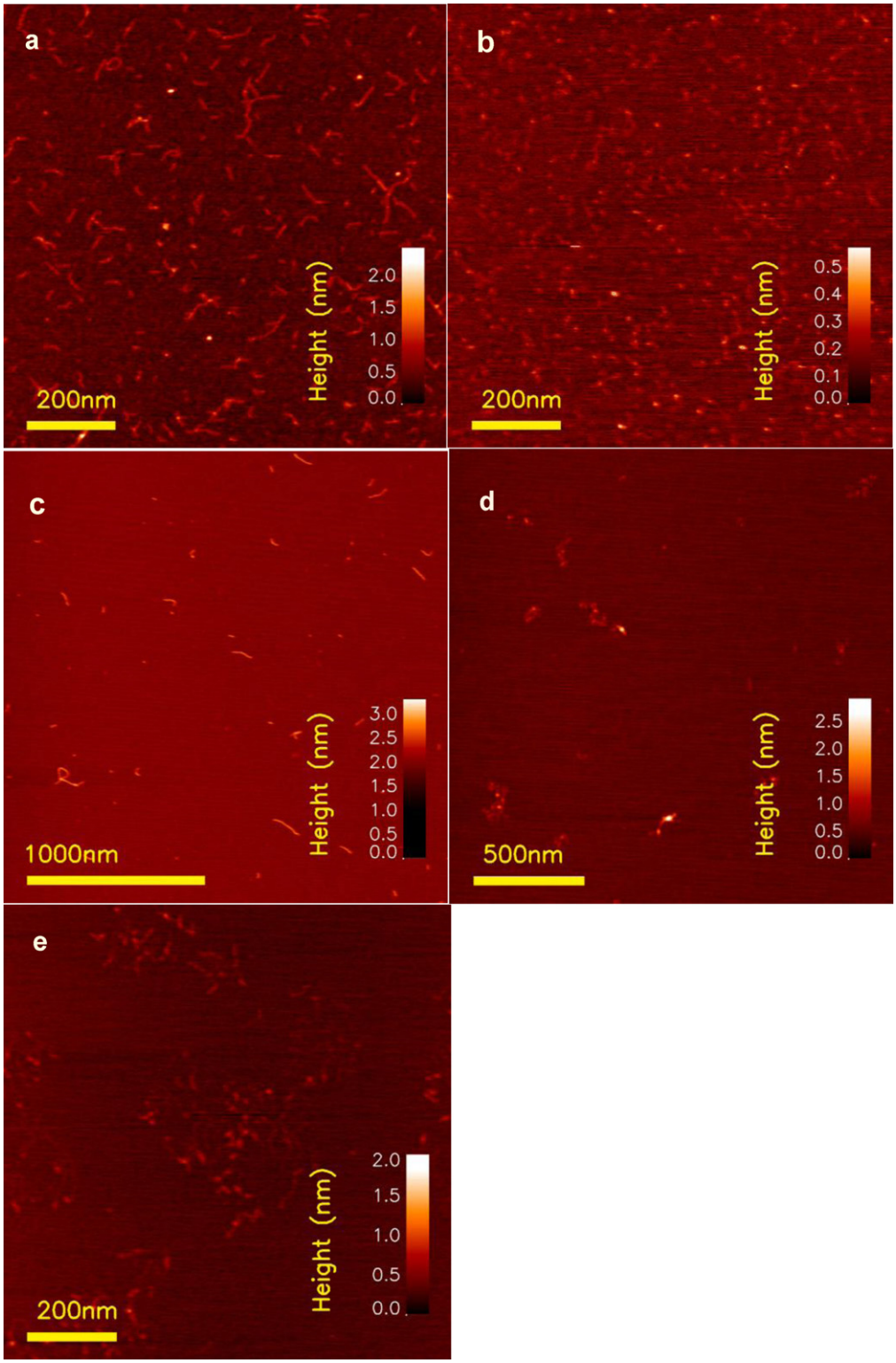

Fig. 4. Tapping mode AFM height topographs of SBG (a), CM-SBG (DS = 0.91) (b), carboxylated scleroglucan ('sclerox-60') (c), and CM-curdlan (DS = 0.4) (d and e). The specimen preparations started from aqueous glycerol only (a–d), and aqueous glycerol with 100 mM NH_4AC (e). The scan size of the topographs shown in a, b and e equals 1 μm × 1 μm, 2 μm × 2 μm for the topograph in d, and 2.5 μm × 2.5 μm for the topograph in c.

as a mixture of triple strands and higher levels of association (aggregation numbers up to 25) (Gawronski et al., 1999). It is therefore reasonable to assume the various aggregation modes observed in SBG are based on the ability to form triple strands, and possibly further associations.

A high molecular weight CM-curdlan (DS = 0.4) was used as a basis for comparison in the AFM study since our previous SEC-MALLS analyses indicated that CM-curdlan (after reducing the chain length to correspond to that of SBG) in aqueous solution behaved as a randomly coiled single chain similar to CM-SBG

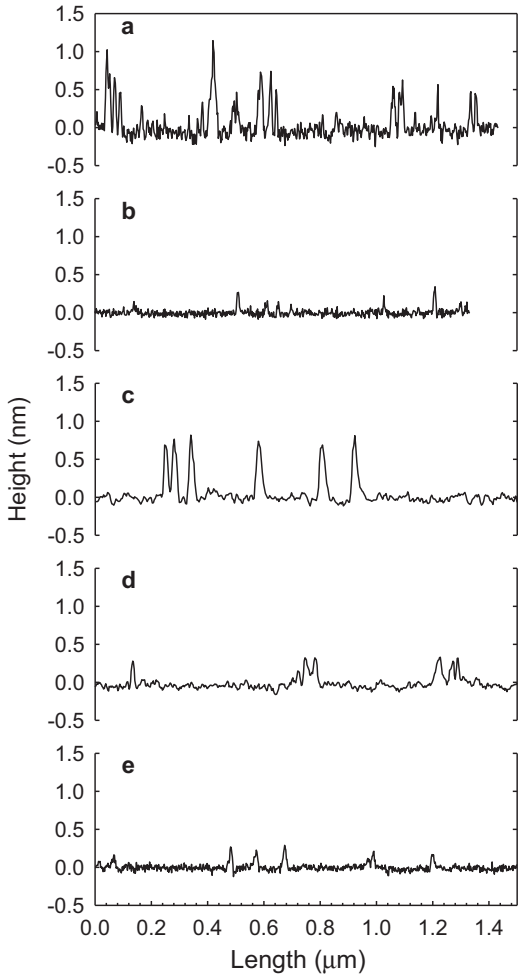

Fig. 5. Cross-sectional analyses of AFM data of SBG (a), CM-SBG with (DS = 0.91) (b), carboxylated scleroglucan ('sclerox-60') (c), and CM-curdlan (DS = 0.4) (d and e) determined from AFM height topographs in Fig. 4. The specimen preparations started from aqueous glycerol only (a–d), or aqueous glycerol with 100 mM NH_4AC (e).

(Qin et al., 2012). However, Fig. 4d shows that high molecular weight CM-curdlan may adopt a necklace-like shape with compact beads. AFM images of CM-curdlan prepared from 100 mM NH_4Ac (Fig. 4e) were to some extent similar to those prepared from pure water (Fig. 4d), but the former also had thicker domains ('beads') that were separated by thinner parts. This behaviour is similar to that described by Kiriy et al. (2002) for two synthethic polyelectrolytes, where the diameter of the beads increased with increasing of ionic strength, while the length of necklaces and the number of beads decreased.

For high molecular weight CM-curdlan in water, extended coils and necklaces with different amounts of beads seem to coexist, whereas low molecular weight CM-curdlan according to both SEC-MALLS (Qin et al., 2012) is single-stranded. Jin, Zhang, Yin, and Nishinari (2006) reported that CM-curdlan with DS as high as 0.83 remained triple-helical when studied by AFM following dissolution in water. Higher DS will normally favour disordering based on standard polyelectrolyte theory, and the discrepancy remains to be explained. The solution properties of CM-curdlan thus seem to be more complex than anticipated and may depend on DS and molecular weight in a manner which remains to be fully elucidated.

The pronounced tendency for (1→3)-β-D-glucans of the SBG-type to form aggregates and particulate materials poses challenges regarding their physical and biological characterisation, but provides on the other hand possibilities to tailor SBG solutions and dispersions through manipulation of the aggregation processes, for example through temperature or pH variations.

4.2. Methodical considerations

Dynamic light scattering analyses reveal the hydrodynamic size distributions of SBG solutions. As expected for a partially and possibly metastable system a broad distribution is obtained. The multimodality (Figs. 1 and 2) may be considered as simplifications as the CONTIN analysis groups the data into a minimum number of discrete components (Provencher, 1982). Nevertheless, the influence of temperature and removal of larger particles by centrifugation is clear. Interestingly, the SBG system shows thermal hysteresis as the downward shift in particle size distribution by heating is not reversed by cooling. Moreover, the reduction in particle size by heating parallels the melting behaviour observed by rheological measurements at higher concentrations (Qin et al., 2012). Nevertheless, both the reduction of aggregate particle size and the melting of SBG gels are probably not related to destabilisation of triple-stranded structures, as extensive chain association has been observed to persist at much higher temperatures.

Ultramicroscopy imaging of polysaccharide has been developed as a valuable tool in providing information related to conformational states of polysaccharides. Examples of this include assessment of chain stiffness (Stokke & Brant, 1990; Stokke, Elgsaeter, Skjåk-Bræk, & Smidsrød, 1987), strandedness of polysaccharides undergoing a conformational transition (Stokke, Elgsaeter, Hara, Kitamura, & Takeo, 1993; Stokke, Smidsrød, & Elgsaeter, 1989), linear to macrocycle conversion and supercoiling associated with that (Stokke, Elgsaeter, Brant, & Kitamura, 1991; Stokke, Elgsaeter, Brant, Kuge, & Kitamura, 1993) and dissociation of triplex structures associated with chemical modification (Stokke et al., 2001). These phenomena are all assessed based on preparation techniques that preserve some relevant conformational features to the state subjected to imaging (Stokke & Brant, 1990).

A crucial step in preparation of dry specimens for ultramicroscopy imaging is the drying step, which may influence the chains conformation of the specimens in the images (Stokke & Elgsaeter, 1994). The observation by AFM of apparently triple-stranded structures in CM-curdlan with a DS as high as 0.83 (Jin et al., 2006) may possibly be attributed to chain aggregation induced by the use of air-drying rather than of vacuum-drying, which is preferred in this method.

There are several conditions that we should know before we choose the real images to analysis. First, the sample solution needs to be prepared at proper conditions without degrading or changing its chain conformation (for example triple into single chains, or vice versa). Secondly, spraying onto the substrate must be performed at sufficiently low concentrations to allow distinction between concentration effects and chain associations in the interpretation of observed overlapping chains. It is further important to assess whether the chains retain their macromolecular properties upon adsorption to the mica and in the subsequent drying step.

5. Conclusions

Dilute SBG solutions were studied using DLS and AFM and compared to CM-SBG and also other (1→3)-β-D-glucans, including CM-curdlan and sclerox-60. Depending on the sample treatment a wide range of structures are formed. Single chains may co-exist with triple-stranded structures and even larger particulate structures. The data are in good agreement with previous studies using SEC-MALLS and rheology.

The use of high molecular weight CM-curdlan (DS = 0.4) as a reference material resulted in observations of anomalous behaviour

in AFM which only to some extent can be explained by the high molecular weight compared to SBG and CM-SBG.

Acknowledgments

Dr. Erik Steene, Biotec Pharmacon, Tromsø, Norway, is thanked for providing glucan batches, and for fruitful discussions. Katarzyna Maria Psonka-Antonczyk is thanked for knowledge sharing in AFM. The project was supported by the Research Council of Norway (Grant 182695/I40).

References

Bluhm, T. L., Deslandes, Y., Marchessault, R. H., Pérez, S., & Rinaudo, M. (1982). Solid-state and solution conformation of scleroglucan. *Carbohydrate Research*, *100*, 117–130.

Bluhm, T. L., & Sarko, A. (1977). The triple helical structure of lentinan, a linear (1→3)-β-D-glucan. *Canadian Journal of Chemistry*, *55*, 293–299.

Bohn, J. A., & BeMiller, J. N. (1995). (1→3)-β-D-Glucans as biological response modifiers: a review of structure-functional activity relationships. *Carbohydrate Polymers*, *28*, 3–14.

Burchard, W. (1991). Static and dynamic light scattering approaches to structure determination of biopolymers. In S. E. Harding, D. B. Satelle, & V. A. Bloomfield (Eds.), *Laser light scattering in biochemistry* (pp. 3–22). Cambridge: The Royal Society of Chemistry.

Carbonero, E. R., Sassaki, G. L., Stuelp, P. M., Gorin, P. A. J., Woranovicz-Barreira, S. M., & Iacomini, M. (2001). Comparative studies of the polysaccharides isolated from lichenized fungi of the genus Cladonia: significance as chemotypes. *FEMS Microbiology Letters*, *194*, 65–69.

Deslandes, Y., Marchessault, R. H., & Sarko, A. (1980). Triple-helical structure of (1→3)-β-D-glucan. *Macromolecules*, *13*, 1466–1471.

Falch, B. H., & Stokke, B. T. (2001). Structural stability of (1→3)-β-D-glucan macrocycles. *Carbohydrate Polymers*, *44*, 113–121.

Fang, Y., Spisz, T. S., Wiltshire, T., D'Costa, N. P., Bankman, I. N., Reeves, R. H., et al. (1998). Solid-state DNA sizing by atomic force microscopy. *Analytical Chemistry*, *70*, 2123–2129.

Gawronski, M., Park, J. T., Magee, A. S., & Conrad, H. (1999). Microfibrillar structure of PGG-glucan in aqueous solution as triple-helix aggregates by small angle X-ray scattering. *Biopolymers*, *50*, 569–578.

Guo, B., Elgsaeter, A., Christensen, B. E., & Stokke, B. T. (1998). Sclerox-chitosan cogels: effects of charge density on swelling of gels in ionic aqueous solution and in poor solvents, and on the rehydration of dried gels. *Polymer Gels and Networks*, *6*, 471–492.

Huang, H., Ostroff, G. R., Lee, C. K., Agarwal, S., Ram, S., Rice, P. A., et al. (2012). Relative contributions of dectin-1 and complement to immune responses to particulate β-glucans. *The Journal of Immunology*, *189*, 312–317.

Jin, Y., Zhang, H., Yin, Y., & Nishinari, K. (2006). Comparison of curdlan and its carboxymethylated derivative by means of rheology, DSC, and AFM. *Carbohydrate Research*, *341*, 90–99.

Kiriy, A., Gorodyska, G., Minko, S., Jaeger, W., Štěpánek, P., & Stamm, M. (2002). Cascade of coil-globule conformational transitions of single flexible polyelectrolyte molecules in poor solvent. *Journal of the American Chemical Society*, *124*, 13454–13462.

Laugier, O. B., Spasić, S. D., Mandić, V., Jakovljević, D., & Vrvić, M. M. (2012). The effects of repetitive alkaline/acid extractions of *Saccharomyces cerevisiae* cell wall on antioxidative and bifidogenic efficacy. *International Journal of Food Science & Technology*, *47*, 369–375.

McIntire, T. M., & Brant, D. A. (1998). Observations of the (1→3)-β-D-glucan linear triple helix to macrocycle interconversion using noncontact atomic force microscopy. *Journal of the American Chemical Society*, *120*, 6909–6919.

McIntosh, M., Stone, B., & Stanisich, V. (2005). Curdlan and other bacterial (1→3)-β-D-glucans. *Applied Microbiology and Biotechnology*, *68*, 163–173.

Palma, A. S., Feizi, T., Zhang, Y., Stoll, M. S., Lawson, A. M., Díaz-Rodríguez, E., et al. (2006). Ligands for the β-glucan receptor, dectin-1, assigned using designer microarrays of oligosaccharide probes (neoglycolipids) generated from glucan polysaccharides. *Journal of Biological Chemistry*, *281*, 5771–5779.

Provencher, S. W. (1982). A constrained regularization method for inverting data represented by linear algebraic or integral equations. *Computer Physics Communications*, *27*, 213–227.

Qin, F., Aachmann, F. L., & Christensen, B. E. (2012). Chain length distribution and aggregation of branched (1→3)-β-D-glucans from *Saccharomyces cerevisae*. *Carbohydrate Polymers*, *90*, 1092–1099.

Read, S. M., Currie, G., & Bacic, A. (1996). Analysis of the structural heterogeneity of laminarin by electrospray-ionisation-mass spectrometry. *Carbohydrate Research*, *281*, 187–201.

Sletmoen, M., Christensen, B. E., & Stokke, B. T. (2005). Probing macromolecular architectures of nanosized cyclic structures of (1→3)-β-D-glucans by AFM and SEC-MALLS. *Carbohydrate Research*, *340*, 971–979.

Sletmoen, M., & Stokke, B. T. (2008). Higher order structure of (1,3)-β-D-glucans and its influence on their biological activities and complexation abilities. *Biopolymers*, *89*, 310–321.

Stokke, B. T., & Brant, D. A. (1990). The reliability of wormlike polysaccharide chain dimensions estimated from electron micrographs. *Biopolymers*, *30*, 1161–1181.

Stokke, B. T., & Elgsaeter, A. (1994). Conformation, order–disorder conformational transitions and gelation of non-crystalline polysaccharides studied using electron microscopy. *Micron*, *25*, 469–491.

Stokke, B. T., Elgsaeter, A., Brant, D. A., & Kitamura, S. (1991). Supercoiling in circular triple-helical polysaccharides. *Macromolecules*, *24*, 6349–6351.

Stokke, B. T., Elgsaeter, A., Brant, D. A., Kuge, T., & Kitamura, S. (1993). Macromolecular cyclization of (1→6)-branched-(1→3)-β-D-glucans observed after denaturation–renaturation of the triple-helical structure. *Biopolymers*, *33*, 193–198.

Stokke, B. T., Elgsaeter, A., Hara, C., Kitamura, S., & Takeo, K. (1993). Physicochemical properties of (1→6)-branched (1→3)-β-D-glucan. 1. Physical dimensions estimated from hydrodynamic and electron microscopic data. *Biopolymers*, *33*, 561–573.

Stokke, B. T., Elgsaeter, A., Skjåk-Bræk, G., & Smidsrød, O. (1987). The molecular size and shape of xanthan, xylinan, bronchial mucin, alginate, and amylose as revealed by electron microscopy. *Carbohydrate Research*, *160*, 13–28.

Stokke, B. T., Falch, B. H., & Dentini, M. (2001). Macromolecular triplex zipping observed in derivatives of fungal (1→3)-β-D-glucan by electron and atomic force microscopy. *Biopolymers*, *58*, 535–547.

Stokke, B. T., Smidsrød, O., & Elgsaeter, A. (1989). Electron microscopy of native xanthan and xanthan exposed to low ionic strength. *Biopolymers*, *28*, 617–637.

Striegel, A., & Timpa, J. D. (1995). Molecular characterization of polysaccharides dissolved in Me_2NAc–LiCl by gel-permeation chromatography. *Carbohydrate Research*, *267*, 271–290.

Striegel, A. M., & Timpa, J. D. (1996). Size exclusion chromatography of polysaccharides in dimethylacetamide–lithium chloride. *ACS Symposium Series*, *635*, 366–378.

Vetvicka, V., Vashishta, A., Saraswat-Ohri, S., & Vetvickova, J. (2008). Immunological effects of yeast- and mushroom-derived beta-glucans. *Journal of Medicinal Food*, *11*, 615–622.

Williams, D. L., McNamee, R. B., Jones, E. L., Pretus, H. A., Ensley, H. E., Browder, I. W., et al. (1991). A method for the solubilization of a (1→3)-β-D-glucan isolated from *Saccharomyces cerevisiae*. *Carbohydrate Research*, *219*, 203–213.

Yanaki, T., Ito, W., Tabata, K., Kojima, T., Norisuye, T., Takano, N., et al. (1983). Correlation between the antitumor activity of a polysaccharide schizophyllan and its triple-helical conformation in dilute aqueous solution. *Biophysical Chemistry*, *17*, 337–342.

Yanaki, T., & Norisuye, T. (1983). Triple helix and random coil of scleroglucan in dilute-solution. *Polymer Journal*, *15*, 389–396.

Zhang, L., Ding, Q., Zhang, P., Zhu, R., & Zhou, Y. (1997). Molecular weight and aggregation behaviour in solution of β-D-glucan from *Poria cocos* sclerotium. *Carbohydrate Research*, *303*, 193–197.

Zhang, L., & Yang, L. (1995). Properties of *auricularia auricula-judae* β-D-glucan in dilute solution. *Biopolymers*, *36*, 695–700.